

## Research Article

# Degradation of Tannic Acid Using $\text{TiO}_2$ Nanotubes as Electrocatalyst

**N. Lakshmi Kruthika, G. Bhaskar Raju, and S. Prabhakar**

*National Metallurgical Laboratory, Madras Centre, CSIR Madras Complex, Taramani, Chennai 600113, India*

Correspondence should be addressed to G. Bhaskar Raju; [gbraju55@gmail.com](mailto:gbraju55@gmail.com)

Received 12 August 2013; Revised 1 November 2013; Accepted 1 December 2013; Published 5 January 2014

Academic Editor: Patrick S. M. Dunlop

Copyright © 2014 N. Lakshmi Kruthika et al. This is an open access article distributed under the Creative Commons Attribution License, which permits unrestricted use, distribution, and reproduction in any medium, provided the original work is properly cited.

Structured  $\text{TiO}_2$  nanotubes were grown on 2 mm thick titanium sheet by anodization of titanium in ethylene glycol medium containing 0.025 M NaF. The morphology of  $\text{TiO}_2$  nanotubes (TNT) was characterized using field emission scanning electron microscope. The potential of TNT as anode and also as photocatalyst for the degradation of tannic acid was studied. The mineralization of tannic acid was measured in terms Total Organic Carbon (TOC). Only 50% of TOC could be removed by exposing the tannic acid solution to UV-radiation (photolysis), whereas it was improved to 70% by electrooxidation (EO) using TNT as anode. Maximum degradation of 83% was achieved when electrooxidation was conducted under the influence of UV-radiation (photoelectrocatalytic process (PEC)). Among the electrolytes tried,  $\text{Na}_2\text{SO}_4$  was observed to be very effective for the degradation of tannic acid. The kinetics of tannic acid degradation by photoelectrocatalytic process was found to follow zero-order rate expression.

## 1. Introduction

Recent researchers have demonstrated the treatment of wastewater containing toxic and refractory organic pollutants by electrochemical and photocatalytic methods. The photocatalytic activity of  $\text{TiO}_2$  nanoparticles for the degradation of organics was found to be encouraging [1, 2]. The  $\text{TiO}_2$  nanoparticles were also tried in various applications like hydrogen sensors [3], solar cells [4], and biocompatible materials [5]. Because of superior photocatalytic activity, the  $\text{TiO}_2$  nanofilms were also attempted for the degradation of dyes, detergents, and organic acids [6]. Since the properties of the materials vary with their microstructure, the nanotubes are expected to perform much better than the commercially available  $\text{TiO}_2$  powders. Variety of techniques such as hydrothermal, template synthesis, magnetic sputtering, and sol-gel have been tried for the synthesis of nanoscaled  $\text{TiO}_2$  wires, dots, particulates, and tubes [7]. Preparation of titanium nanotubes (TNT) by chemical precursor route fails to control the thickness and shape of the nanotubes. On the other hand, precise control over the nanotube wall thickness could be

achieved by template method. The potentiostatic anodization technique was found to yield highly ordered titanium nanotubes with uniform wall thickness. The shape, wall thickness, and length of the nanotubes are easily controlled by electrolyte and applied voltage. Albu et al. [8] modified the applied voltage to prepare new bamboo type titanium nanotubes and Ji et al. [9] used alternating voltage to produce double walled titanium nanotubes. Very recently, titanium nanotubes having structures like bamboo leaves, squares, triangles, and flowers were achieved by varying the parameters [10, 11]. The potentiostatic anodization of titanium plate is considered advantageous because TNT could be grown directly on the substrate. The  $\text{TiO}_2$  nanoparticles prepared by other methods are just deposited on the substrate unlike titanium nanotubes which are directly bound to Ti substrate. The nanotubular microstructures are perpendicular to the electrically conductive Ti substrate, forming a Schottky-type contact [7] thereby providing two separate channels for efficient electron and positive hole transport from interface to electrode. This is in sharp contrast to electron hopping in  $\text{TiO}_2$  nanoparticles, which were widely used as electron accepting species in dye

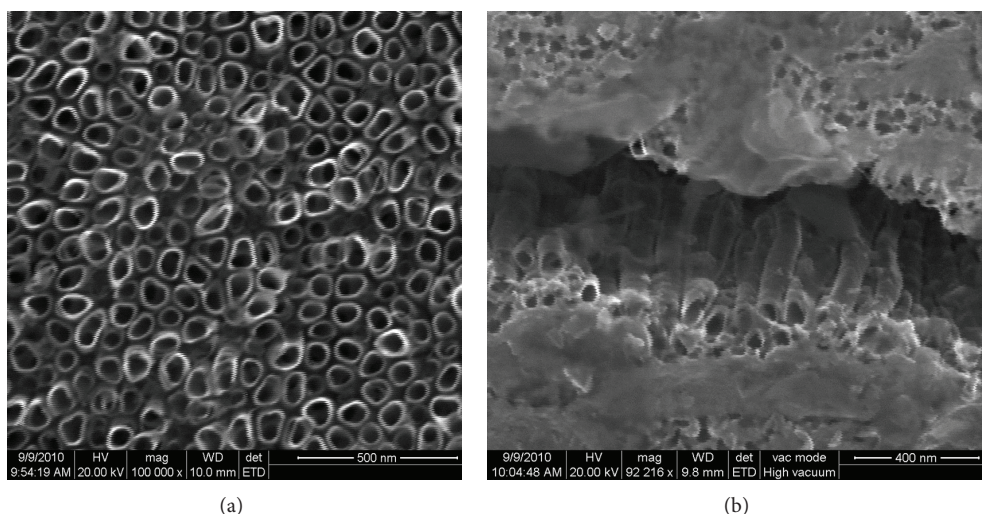


FIGURE 1: (a) Top view and (b) cross-sectional FESEM images of the  $\text{TiO}_2$  nanotube arrays.

sensitized solar cells [12]. Moreover, the ordered tube like architecture can provide unidirectional electric channel for superior charge separation and charge transport. Further, the  $\text{TiO}_2$  nanotubes prepared by anodization technique have better anatase to rutile ratio which enhances the electrocatalytic property. The oxidation of acetaldehyde [13], glucose, dopamine, ascorbic acid, and hydrazine [14] was studied using TNT electrode. It was reported that the photocatalytic activity and photodegradation can be enhanced by incorporating minor amount of active carbon in TNT electrodes [15]. The degradation of humic acid was observed to be better by photoelectrocatalytic process compared to conventional photocatalytic method. The humic acid was selectively removed before chlorine generation by using TNT photoanode [16]. The photoelectrocatalytic degradation of methyl orange dye [17], Disperse Orange 1, Disperse Red 1, and Disperse Red 13 [18] using TNT electrode, was also investigated and found to be advantageous than simple photocatalytic method.

In this paper, the degradation of tannic acid was studied by photolysis, electrooxidation, and photoelectrocatalytic process using TNT electrode. Tannic acid was considered because it is toxic to aquatic organisms such as algae, phytoplankton, fish, and invertebrates [19, 20] and highly refractive to conventional degradation. Also tannic acid can form metal complexes which could alter the aquatic ecosystem [21].

## 2. Experimental Materials and Methods

**2.1. Materials.** All the chemicals used in the present study were of analytical grade. Double distilled water free from organic carbon was employed for all the experiments. The pH of the aqueous solutions was adjusted using dilute  $\text{H}_2\text{SO}_4$  and NaOH solutions.

**2.2. Preparation of TNT Electrode.** The  $\text{TiO}_2$ -nanotube arrays were grown on Ti sheet by anodization method [22]. Titanium sheet (2 mm thick) was cut into  $2 \times 2$  cm pieces and

mirror polished using abrasive sheets of different grain size and then ultrasonically degreased using deionized water and finally in 1:1 mixture of acetone and ethanol before drying in air stream. These sheets were anodized using 95% ethylene glycol (99% purity) and 0.025 M NaF electrolyte. The electrolysis experiments were conducted using a potentiostat/galvanostat system (Model-KM064, K-Pas Instronics Engineers, India). The electrodes were connected to the respective terminals of the potentiostat and the anodization was continued at a constant current for a period of six hours by keeping the voltage at 20 V. For better templating of nanotubes with Ti-substrate, the titanium sheet was etched in Kroll's reagent ( $\text{HF}:\text{HNO}_3:\text{H}_2\text{O}$ ) for 30 seconds just before anodizing. Platinum foil was used as counter electrode in all the experiments. The distance between the two electrodes was maintained at 1.0 cm. The temperature of the electrolytic bath was maintained between 15 and  $20^\circ\text{C}$  and the solution was kept under agitation with the help of magnetic stirrer. After anodization, the samples were washed with water and ultrasonicated in acetone to remove surface debris (precipitate falling out of solution). The anodized amorphous  $\text{TiO}_2$  nanotubes were annealed at  $480^\circ\text{C}$  in oxygen atmosphere for six hours with heating and cooling rate of  $1^\circ\text{C min}^{-1}$  to obtain crystallized samples. The morphology and array of nanotubes were studied using field emission scanning electron microscope. Top view and side view of Ti nanotubes are presented in Figure 1. The SEM images indicate that the average diameter and wall thickness of the nanotubes are around 80 nm and 15 nm, respectively. Similar results have been reported earlier with ethylene glycol as the medium [23]. The height/length of each tube is observed to be more than 500 nm.

**2.3. Experimental Setup.** The high pressure mercury vapor lamp (HML-LP 88) which emits a monochromatic light of 365 nm was used as radiation source. The sample holder made of silica glass of the photoreactor was slightly modified to have

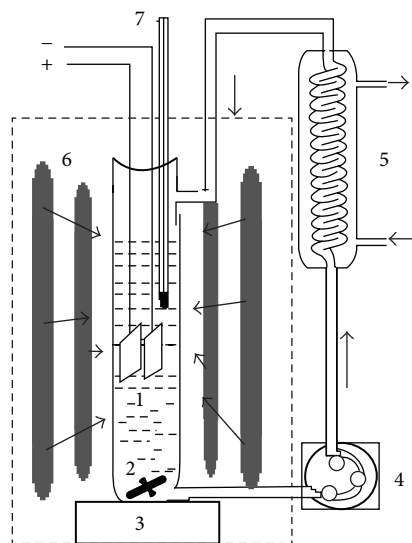


FIGURE 2: Experimental setup: (1) reactor tube, (2) magnetic paddle, (3) magnetic stirrer, (4) peristaltic pump, (5) cooling condenser, (6) UV-radiation, (7) electrode leads.

an inlet and outlet, so that the experimental solution can be recirculated. The light power inside the reactor was measured using the energy meter (OPHIR, NOVA make) and it was observed to be 130 microwatts. The solution was circulated through the cooling condenser to the reactor by peristaltic pump. Cold water was continuously passed through the inlet of the condenser jacket and let out through the outlet. The temperature of the tannin solution was maintained around 25°C. The tannin solution was kept in agitation by the bubbles generated by electrolysis and by its recirculation. In addition to this, magnetic stirrer was also used for thorough mixing of the contents. The surface area of TNT anode exposed to electrolysis was estimated to be 4.07 cm<sup>2</sup>. Platinum was used as cathode and the gap between anode and cathode was maintained at 0.5 cm. The schematic diagram of experimental setup is shown in Figure 2. Prior to each experiment, the working electrode was anodically polarized for 60 seconds in 0.01 M H<sub>2</sub>SO<sub>4</sub> electrolyte solution at constant current of 100 mA, while Pt electrode was soaked in concentrated HNO<sub>3</sub> for 10 minutes to remove any impurities deposited on the surface.

**2.4. Analysis.** During the course of the experiment, samples (2.0 mL) were collected at regular intervals and analyzed by TOC analyzer (Shimadzu VCSN/CPN Model). The homogenized diluted sample was injected into the reaction chamber packed with catalyst. The carbon is oxidized to CO<sub>2</sub> in the reaction chamber and the CO<sub>2</sub> gas generated is quantitatively estimated by nondispersive infrared analyzer. The TOC was deduced from the measurements of total carbon and inorganic carbon.

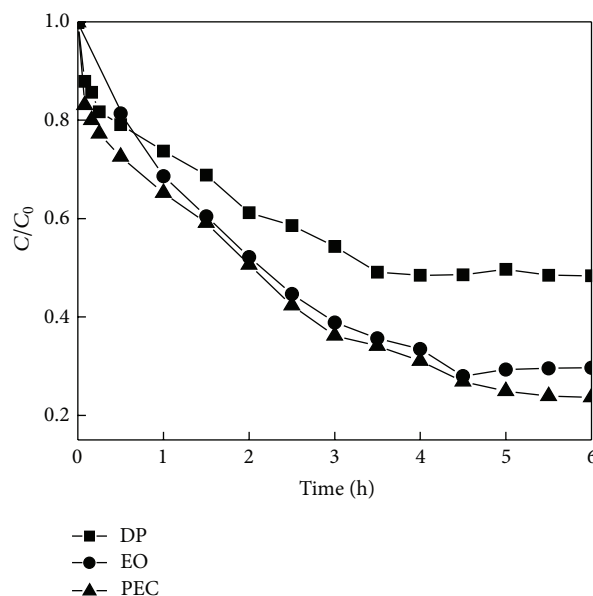


FIGURE 3: Degradation of tannic acid by electrooxidation, direct photolysis, and photoelectrocatalytic process (initial concentration of tannic acid ( $C_0$ ): 100 mg L<sup>-1</sup>, current density: 36.85 mA/cm<sup>2</sup>).

### 3. Results and Discussion

**3.1. Tannic Acid Degradation by Various Techniques.** Degradation of tannic acid by electrooxidation (EO) using TNT electrode as anode, photolysis (DP), and photoelectrocatalytic process (PEC) that is electrooxidation under UV radiation (with  $\lambda$  value of 365 nm) was followed over a period of 6 hours and the results are presented in Figure 3. The cell voltage (open circuit) was measured to be 9.0 V during electrolysis. The potential of the working electrode is 1.31 V versus SCE. From the results, it is apparent that only 50% of TOC could be removed when the tannic acid solution was exposed to UV radiation alone (photolysis). The removal of tannic acid was improved to 70% by electrooxidation (EO) process using TNT as anode. Electrooxidation was carried out in 0.1 M Na<sub>2</sub>SO<sub>4</sub> electrolyte solution at a current density of 36.85 mA/cm<sup>2</sup>. The degradation of tannic acid was improved further (83%) by photoelectrocatalytic process (PEC). It may be attributed to the enhanced generation of photon holes on TiO<sub>2</sub> nanotubes under the combined effect of UV radiation and electrolysis.

Better degradation in the presence of TNT electrode may also be attributed to the higher band gap energy and surface area. Because of high band gap energy, generation of powerful photocarriers is expected when exposed to UV light. Further, the specific surface area of TiO<sub>2</sub> nanotubes is several folds more than the normal electrode and hence adsorbs more organic matter for degradation. Considering the dia and length of each TiO<sub>2</sub> nanotube as  $40 \times 10^{-7}$  cm and  $50 \times 10^{-7}$  cm, the actual surface area of the TNT electrode was estimated to be 72.4 cm<sup>2</sup>. This is nearly 20 times more than the surface area calculated by taking in to account the length and

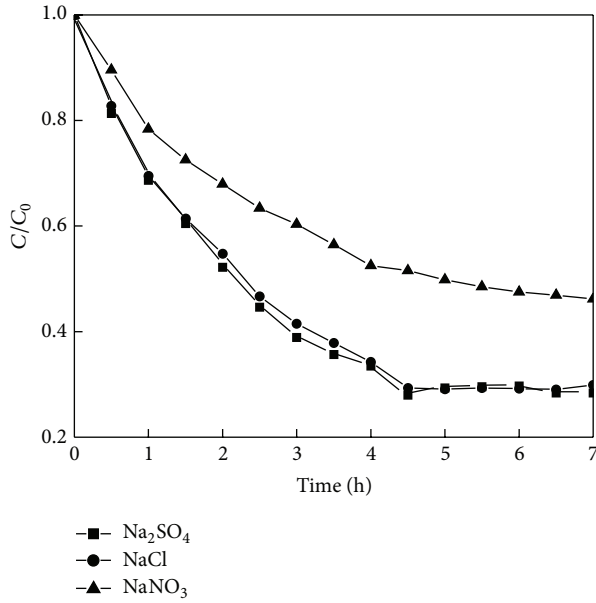


FIGURE 4: Effect of different electrolytes on tannic acid mineralization (initial concentration of tannic acid  $C_0$ :  $100 \text{ mg L}^{-1}$ , current density:  $18.43 \text{ mA cm}^{-2}$ , and electrolyte:  $0.1 \text{ M}$ ).

breadth of the TNT electrode. The large effective surface area is in close proximity with the electrolyte solution, and thus the photogenerated electrons can transfer more effectively to the counter electrode via the external circuit [12]. Thus the enhanced photoelectrochemical activity of the TNT electrode may be attributed due to the effective separation of electron-hole pairs on the surface of the electrode. The special structure and light scattering characteristics may also contribute positively to the transportation of photogenerated holes. Also large number of OH groups available on the surface can prevent the agglomeration of nanotubes. Though better degradation of tannin by PEC process is expected, only marginal improvement was observed. It may be attributed to the formation of stable intermediate compounds that resist degradation even at higher concentration of oxidants. It is known that organic compounds having  $\text{-COOH}$ ,  $\text{-OH}$  (like tannic acid) display high degree of stability because of resonance effect. Thus complete mineralization of compounds like tannic acid appears to be difficult.

**3.2. Effect of Supporting Electrolyte.** Mineralization of tannic acid in the presence of NaCl,  $\text{Na}_2\text{SO}_4$ , and  $\text{NaNO}_3$  electrolytes using TNT electrode was studied by photoelectrocatalytic process. The initial tannic acid concentration of  $100 \text{ mg L}^{-1}$  and applied current density of  $36.86 \text{ mA cm}^{-2}$  were maintained uniformly in all the experiments. From the experimental results presented in Figure 4, it is apparent that the mineralization of tannic acid is effective in the presence of NaCl and  $\text{Na}_2\text{SO}_4$  electrolytes. Better degradation in the presence of NaCl and  $\text{Na}_2\text{SO}_4$  is explained due to the oxidizing species such as  $\text{Cl}_2$ ,  $\text{OCl}^-$ ,  $\text{SO}_4^{\cdot-}$ ,  $\text{S}_2\text{O}_8^{2-}$ , and free radicals produced during electrolysis. It was reported [24, 25] that

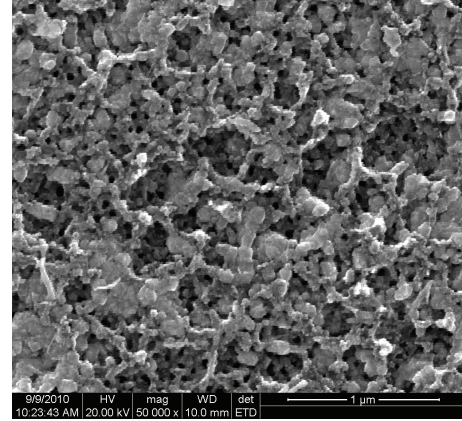
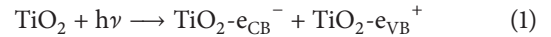
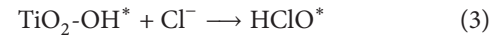


FIGURE 5: SEM images of the TNT electrode after photoelectrocatalytic process in  $0.1 \text{ M}$  NaCl after 30 hours.

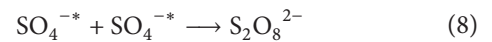
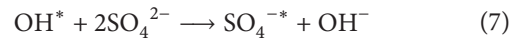
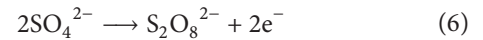
the active chlorine on  $\text{Ti/TiO}_2$  under UV irradiation can be generated as per (1)–(5). The  $\text{OH}^*$  radicals are also produced anodically due to the oxidation of adsorbed water on the electrode surface:



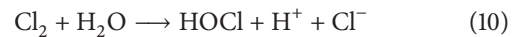
The reaction products  $\text{TiO}_2\text{-e}_{\text{VB}}^+$  and  $\text{TiO}_2\text{-OH}^*$  oxidize chloride ion according to (3) and (4). The adsorbed chloride ions on the semiconductor surface acting as anode could be oxidized by holes generated under UV irradiation. As a result,  $\text{Cl}^*$  and  $\text{HOCl}^*$  are formed:



In the presence of  $\text{Na}_2\text{SO}_4$ , oxidizing agents such as  $\text{OH}^*$ ,  $\text{SO}_4^{\cdot-}$ , and  $\text{S}_2\text{O}_8^{2-}$  are generated according to the reactions:



In addition to the above, oxy chloride species are generated by anodic discharge of chlorine and its reaction with water molecules:



The rate of TOC removal is better at the initial stages of oxidation that is up to 3 hours of electrolysis time. Beyond



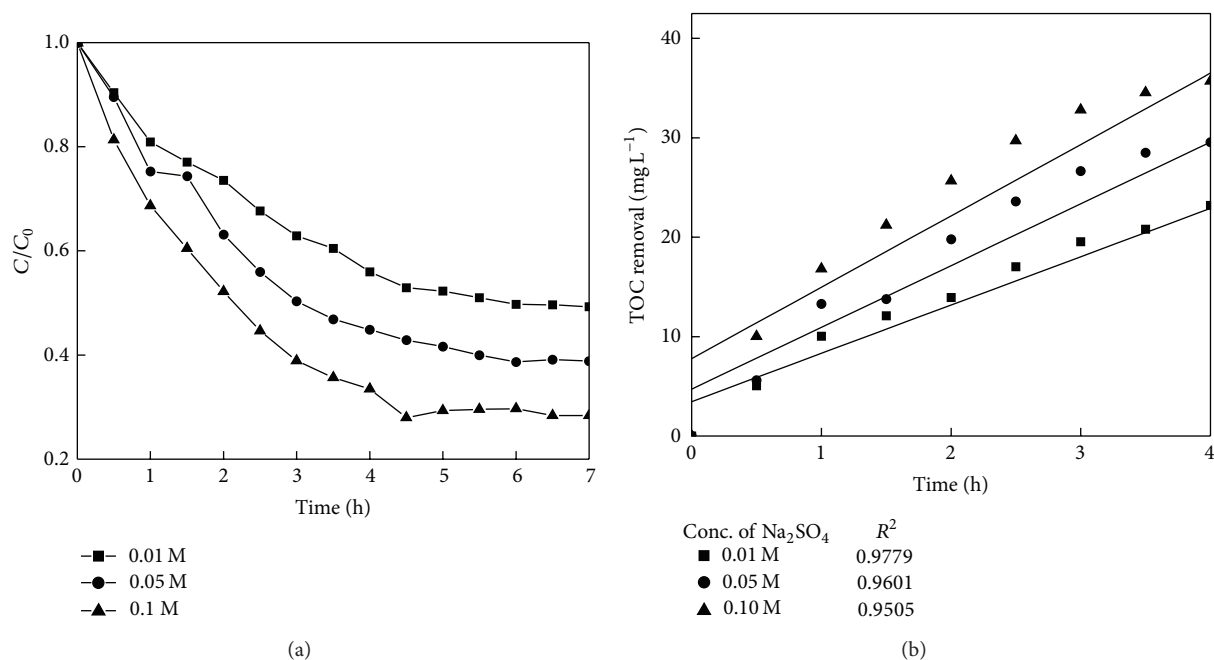


FIGURE 6: (a) Effect of  $\text{Na}_2\text{SO}_4$  concentration and (b) kinetics of the tannic acid mineralization (initial concentration of tannic acid  $C_0$ :  $100 \text{ mg L}^{-1}$ , current density:  $18.43 \text{ mA cm}^{-2}$ ).

this point, the removal was found to be marginal. The slow rate of mineralization at the later stage may be ascribed to mass transfer limitations [26]. The results suggest that the in situ generation of hydroxyl ( $\text{OH}^*$ ), sulfate ( $\text{SO}_4^{*-}$ ) radicals, and  $\text{S}_2\text{O}_8^{2-}$  species plays a vital role in the mineralization of the tannic acid by indirect oxidation. The degradation was observed to be poor in the presence of  $\text{NaNO}_3$  because there is no generation of oxidant from the supporting electrolyte. Though the degradation rate of tannic acid in the presence of  $\text{NaCl}$  was observed to be better, the  $\text{TiO}_2$  nanotube arrays were found to be affected (Figure 5) on a long run. Though it was demonstrated that the  $\text{TiO}_2$  nanotube arrays possess self-cleaning property under UV light [3], the electrode surface was seen fully covered with debris. In the case of phenol degradation, the polymeric products formed during electrooxidation are found to readsorb on electrode surface thus reducing the efficiency of the electrode. The low efficiency due to blocking of electrode surface by pollutant molecules/reaction products and fouling of electrode material is some of the drawbacks of electrooxidation process.

**3.3. Effect of  $\text{Na}_2\text{SO}_4$  Concentration on the Mineralization of Tannic Acid.** The mineralization of tannic acid at different  $\text{Na}_2\text{SO}_4$  concentrations of 0.01, 0.05, and 0.1 M was recorded using photoelectrocatalytic process. Current density of  $18.43 \text{ Ma cm}^{-2}$  and tannic acid concentration of  $100 \text{ mg L}^{-1}$  were maintained uniformly during the experiment. A slight increase of 0.5 V beyond 3 hours of electrolysis may be attributed to the depletion in ionic concentration of  $\text{SO}_4^{2-}$  in the bulk of the electrolyte. From the results presented in Figure 6, it is apparent that the TOC removal increases by increasing the concentration of  $\text{Na}_2\text{SO}_4$ . Thus

the mineralization of tannic acid in the presence of  $\text{Na}_2\text{SO}_4$  suggests the role of mediated oxidants in addition to direct electron transfer reaction at the surface of the anode [27]. From the results shown in Figure 6(b), it is evident that the mineralization of tannic acid by photoelectrocatalytic process follows the zero-order kinetics during the initial stage. This implies that electrooxidation is current control process [28] where the pollutant molecules arrive at the anode faster than the electrochemical production of oxidant. This is particularly so at low current densities and high concentration of pollutant molecules.

**3.4. Effect of Current Density on TOC Removal.** The effect of current density on TOC removal was studied at four different applied current densities, namely, 12.28, 24.56, 36.86, and  $49.14 \text{ mA cm}^{-2}$  by PEC process and the results obtained are plotted in Figure 7(a). From the results it is apparent that the applied current density has marked influence on TOC removal. The TOC removal was found to increase with current density. However, it should be noted that the TOC removal beyond  $36.86 \text{ mA cm}^{-2}$  is very marginal. The TOC removal was observed to be better at initial stage of electrolysis at all current densities. The reduction in TOC was observed to be marginal beyond 4 hours of electrooxidation. The goodness of fit of linear regression ( $R^2$  values) suggests that the process of electrooxidation can be described in terms of zero-order reaction and current controlled [29] during the initial stage.

**3.5. Effect of pH on Mineralization.** Since the initial pH of the electrolyte is an important variable to achieve the total mineralization, the photoelectrocatalysis was carried out in

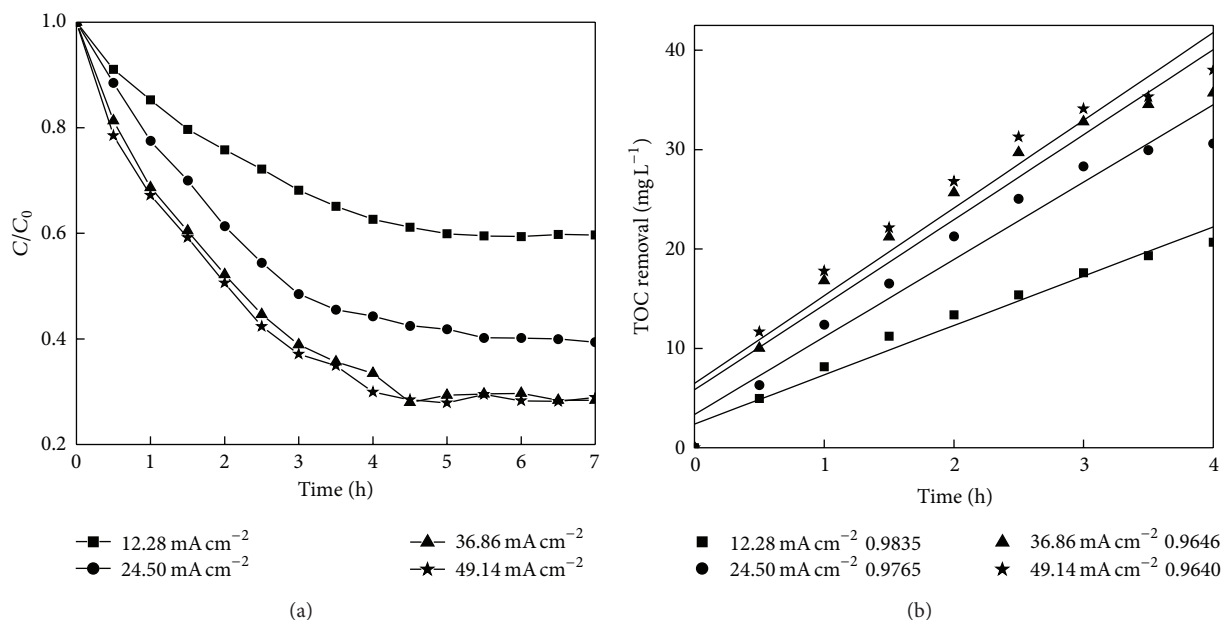


FIGURE 7: (a) Effect of current density on TOC removal and (b) kinetics of tannic acid mineralization (initial concentration of tannic acid  $C_0$ :  $100 \text{ mg L}^{-1}$ ).

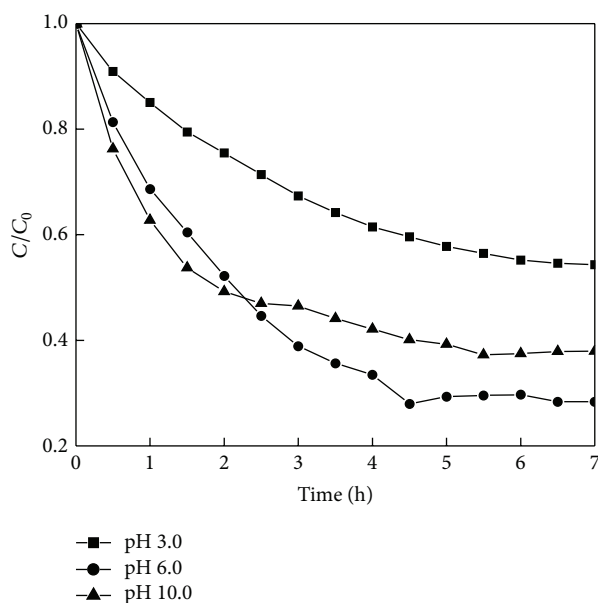
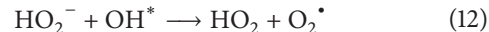


FIGURE 8: Effect of pH on TOC removal (initial concentration of tannic acid  $C_0$ :  $100 \text{ mg L}^{-1}$ , current density:  $18.43 \text{ mA cm}^{-2}$ ,  $0.1 \text{ M Na}_2\text{SO}_4$ ).

acidic, basic, and neutral pH. The effect of initial pH on the depletion of TOC by PEC process using TNT anode in the presence of  $\text{Na}_2\text{SO}_4$  is shown in Figure 8. The TOC removal was observed to be relatively better at pH 6.0. In general, the pH of the electrolyte mostly affects the indirect mediated oxidation. In alkaline condition, the evolution of oxygen is comparatively high and thus prevents the diffusion of pollutant molecule to the electrode surface [30]. Further, inactive

hydroperoxide ( $\text{HO}_2^-$ ) anion which acts as scavenger for  $\text{OH}^*$  is formed in alkaline pH [31]:



It was also observed that the change in pH affects the solubility of the oxygen which may adversely affect the generation of free radicals and mediated oxidants in the bulk electrolyte. At an applied current density of  $36.86 \text{ mA cm}^{-2}$ , energy required for tannic acid mineralization was calculated to be  $2.14 \text{ Wh L}^{-1}$ .

#### 4. Conclusions

Mineralization of tannic acid by direct photolysis, electrooxidation, and photoelectrocatalytic process was studied using TNT electrode. The degradation of tannic acid is only 50% by direct photolysis process, whereas it was improved to 70% by electrooxidation process using TNT as anode. The mineralization of tannic acid was observed to be maximum (83%) by photoelectrocatalytic process. The nature of the electrolyte was found to influence the anodic oxidation of tannic acid. Among the three different electrolytes used during photoelectrocatalytic process,  $\text{Na}_2\text{SO}_4$  and  $\text{NaCl}$  were found to be effective than  $\text{NaNO}_3$ . The electrode surface particularly the array of nanotubes was affected on a long run particularly in the presence of  $\text{NaCl}$ . An increase in the concentration of electrolyte and applied current density was found to increase the degradation of tannic acid. The mineralization is found to be effective under neutral pH. The photoelectrocatalytic process was found to obey zero-order kinetics at the initial stage.

## Conflict of Interests

The authors declare that there is no conflict of interests regarding the publication of this paper.

## Acknowledgments

The authors are thankful to the director of National Metallurgical Laboratory for permission to publish this work. The authors gratefully acknowledge the financial support from NWP-044 Project.

## References

- [1] S. P. Albu, A. Ghicov, J. M. Macak, R. Hahn, and P. Schmuki, "Self-organized, free-standing TiO<sub>2</sub> nanotube membrane for flow-through photocatalytic applications," *Nano Letters*, vol. 7, no. 5, pp. 1286–1289, 2007.
- [2] K. Shankar, G. K. Mor, H. E. Prakasam et al., "Highly-ordered TiO<sub>2</sub> nanotube arrays up to 220  $\mu\text{m}$  in length: use in water photoelectrolysis and dye-sensitized solar cells," *Nanotechnology*, vol. 18, no. 6, Article ID 065707, 2007.
- [3] G. K. Mor, M. A. Carvalho, O. K. Varghese, M. V. Pishko, and C. A. Grimes, "A room-temperature TiO<sub>2</sub>-nanotube hydrogen sensor able to self-clean photoactively from environmental contamination," *Journal of Materials Research*, vol. 19, no. 2, pp. 628–634, 2004.
- [4] M. Paulose, K. Shankar, O. K. Varghese, G. K. Mor, B. Hardin, and C. A. Grimes, "Backside illuminated dye-sensitized solar cells based on titania nanotube array electrodes," *Nanotechnology*, vol. 17, no. 5, pp. 1446–1448, 2006.
- [5] D. Gong, C. A. Grimes, O. K. Varghese et al., "Titanium oxide nanotube arrays prepared by anodic oxidation," *Journal of Materials Research*, vol. 16, no. 12, pp. 3331–3334, 2001.
- [6] X. Quan, S. Yang, X. Ruan, and H. Zhao, "Preparation of titania nanotubes and their environmental applications as electrode," *Environmental Science and Technology*, vol. 39, no. 10, pp. 3770–3775, 2005.
- [7] Y. Liu, J. Li, B. Zhou et al., "Comparison of photoelectrochemical properties of TiO<sub>2</sub>-nanotube- array photoanode prepared by anodization in different electrolyte," *Environmental Chemistry Letters*, vol. 7, no. 4, pp. 363–368, 2009.
- [8] S. P. Albu, D. Kim, and P. Schmuki, "Growth of aligned TiO<sub>2</sub> bamboo-type nanotubes and highly ordered nanolace," *Angewandte Chemie*, vol. 47, no. 10, pp. 1916–1919, 2008.
- [9] Y. Ji, K.-C. Lin, H. Zheng, J.-J. Zhu, and A. C. S. Samia, "Fabrication of double-walled TiO<sub>2</sub> nanotubes with bamboo morphology via one-step alternating voltage anodization," *Electrochemistry Communications*, vol. 13, no. 9, pp. 1013–1015, 2011.
- [10] J. Gong, C. Lin, M. Ye, and Y. Lai, "Enhanced photoelectrochemical activities of a nanocomposite film with a bamboo leaf-like structured TiO<sub>2</sub> layer on TiO<sub>2</sub> nanotube arrays," *Chemical Communications*, vol. 47, no. 9, pp. 2598–2600, 2011.
- [11] B. Chen, K. Lu, and J. A. Geldmeier, "Highly ordered titania nanotube arrays with square, triangular, and sunflower structures," *Chemical Communications*, vol. 47, no. 36, pp. 10085–10087, 2011.
- [12] M. Paulose, K. Shankar, S. Yoriya et al., "Anodic growth of highly ordered TiO<sub>2</sub> nanotube arrays to 134  $\mu\text{m}$  in length," *Journal of Physical Chemistry B*, vol. 110, no. 33, pp. 16179–16184, 2006.
- [13] H. Xu, G. Vanamu, Z. Nie et al., "Photocatalytic oxidation of a volatile organic component of acetaldehyde using titanium oxide nanotubes," *Journal of Nanomaterials*, vol. 2006, Article ID 78902, 8 pages, 2006.
- [14] M. Hosseini and M. Mohsen Momeni, "Preparation and characterization of TiO<sub>2</sub> nanotubular arrays for electrooxidation of organic compounds: effect of immobilization of the noble metal particles," *International Journal of Modern Physics*, vol. 5, pp. 41–48, 2012.
- [15] T. A. Egerton, M. Janus, and A. W. Morawski, "New TiO<sub>2</sub>/C sol-gel electrodes for photoelectrocatalytic degradation of sodium oxalate," *Chemosphere*, vol. 63, no. 7, pp. 1203–1208, 2006.
- [16] H. Selcuk and M. Bekbolet, "Photocatalytic and photoelectrocatalytic humic acid removal and selectivity of TiO<sub>2</sub> coated photoanode," *Chemosphere*, vol. 73, no. 5, pp. 854–858, 2008.
- [17] Y. S. Sohn, Y. R. Smith, M. Misra, and V. (Ravi) Subramanian, "Electrochemically assisted photocatalytic degradation of methyl orange using anodized titanium dioxide nanotubes," *Applied Catalysis B*, vol. 84, no. 3–4, pp. 372–378, 2008.
- [18] M. E. Osugi, M. V. B. Zanoni, C. R. Chenthamarakshan et al., "Toxicity assessment and degradation of disperse azo dyes by photoelectrocatalytic oxidation on Ti/TiO<sub>2</sub> nanotubular array electrodes," *Journal of Advanced Oxidation Technologies*, vol. 11, no. 3, pp. 425–434, 2008.
- [19] J.-H. An and S. Dultz, "Adsorption of tannic acid on chitosan-montmorillonite as a function of pH and surface charge properties," *Applied Clay Science*, vol. 36, no. 4, pp. 256–264, 2007.
- [20] J. Wang, A. Li, L. Xu, and Y. Zhou, "Adsorption of tannic and gallic acids on a new polymeric adsorbent and the effect of Cu(II) on their removal," *Journal of Hazardous Materials*, vol. 169, no. 1–3, pp. 794–800, 2009.
- [21] Z. Varanka, I. Rojik, I. Varanka, J. Nemcsók, and M. Ábrahám, "Biochemical and morphological changes in carp (*Cyprinus carpio* L.) liver following exposure to copper sulfate and tannic acid," *Comparative Biochemistry and Physiology C*, vol. 128, no. 2, pp. 467–478, 2001.
- [22] B. O'Regan and M. Grätzel, "A low-cost, high-efficiency solar cell based on dye-sensitized colloidal TiO<sub>2</sub> films," *Nature*, vol. 353, no. 6346, pp. 737–740, 1991.
- [23] J. Wang and Z. Lin, "Freestanding TiO<sub>2</sub> nanotube arrays with ultrahigh aspect ratio via electrochemical anodization," *Chemistry of Materials*, vol. 20, no. 4, pp. 1257–1261, 2008.
- [24] M. V. B. Zanoni, J. J. Sene, H. Selcuk, and M. A. Anderson, "Photoelectrocatalytic production of active chlorine on nanocrystalline titanium dioxide thin-film electrodes," *Environmental Science and Technology*, vol. 38, no. 11, pp. 3203–3208, 2004.
- [25] L. E. Fraga, M. A. Anderson, M. L. P. M. A. Beatriz, F. M. M. Paschoal, L. P. Romão, and M. V. B. Zanoni, "Evaluation of the photoelectrocatalytic method for oxidizing chloride and simultaneous removal of microcystin toxins in surface waters," *Electrochimica Acta*, vol. 54, no. 7, pp. 2069–2076, 2009.
- [26] B. Marselli, J. Garcia-Gomez, P.-A. Michaud, M. A. Rodrigo, and C. Comninellis, "Electrogeneration of hydroxyl radicals on boron-doped diamond electrodes," *Journal of the Electrochemical Society*, vol. 150, no. 3, pp. D79–D83, 2003.
- [27] M. Murugananthan, S. S. Latha, G. Bhaskar Raju, and S. Yoshihara, "Role of electrolyte on anodic mineralization of atenolol at boron doped diamond and Pt electrodes," *Separation and Purification Technology*, vol. 79, no. 1, pp. 56–62, 2011.

- [28] S. Li, D. Bejan, M. S. McDowell, and N. J. Bunce, "Mixed first and zero order kinetics in the electrooxidation of sulfamethoxazole at a boron-doped diamond (BDD) anode," *Journal of Applied Electrochemistry*, vol. 38, no. 2, pp. 151–159, 2008.
- [29] S. Yoshihara and M. Murugananthan, "Decomposition of various endocrine-disrupting chemicals at boron-doped diamond electrode," *Electrochimica Acta*, vol. 54, no. 7, pp. 2031–2038, 2009.
- [30] L. Szpyrkowicz, C. Juzzolino, S. N. Kaul, S. Daniele, and M. D. de Faveri, "Electrochemical oxidation of dyeing baths bearing disperse dyes," *Industrial and Engineering Chemistry Research*, vol. 39, no. 9, pp. 3241–3248, 2000.
- [31] S. K. Bhargava, J. Tardio, J. Prasad, K. Föger, D. B. Akolekar, and S. C. Grocott, "Wet oxidation and catalytic wet oxidation," *Industrial and Engineering Chemistry Research*, vol. 45, no. 4, pp. 1221–1258, 2006.



